SAND2017-7417C

Correlation of a Bipolar-Transistor-Based Neutron Displacement Damage Sensor Methodology with Proton Irradiations

Andrew M. Tonigan, *Member, IEEE*, Charles N. Arutt, *Member, IEEE*, Edward J. Parma, Patrick J. Griffin, *Member, IEEE*, Daniel M. Fleetwood, *Fellow, IEEE*, and Ronald D. Schrimpf, *Fellow, IEEE*

***Abstract*—A bipolar-transistor-based sensor technique has been used to compare silicon displacement damage from known and unknown neutron energy spectra generated in nuclear reactor and high-energy-density physics environments. The technique has been shown to yield 1-MeV(Si) equivalent neutron fluence measurements comparable to traditional neutron activation dosimetry. This study significantly extends previous results by evaluating three types of bipolar devices utilized as displacement damage sensors at a nuclear research reactor and at a Pelletron particle accelerator. Ionizing dose effects are compensated for via comparisons with 10-keV x-ray and/or cobalt-60 gamma ray irradiations. Non-ionizing energy loss calculations adequately approximate the correlations between particle-device responses and provide evidence for the use of one particle type to screen the sensitivity of the other.**

***Index Terms*—displacement damage, silicon bipolar transistors, non-ionizing energy loss, ionizing dose, neutron dosimetry, commercial-off-the-shelf parts**

I. Introduction

SINCE Eugene Wigner's work with the Chicago pile nuclear reactor [1], the effects of atoms being displaced by energetic particle bombardment on material properties have been studied. Silicon and other electronic materials are of specific interest due to the interdependence of electronic states and atomic configurations as well as the desirability of using electronic systems in energetic particle environments, e.g., space, experimental physics, nuclear power, etc. Determining the sensitivity of electronic systems to radiation that induces displacement damage is performed through a combination of simulation and experiment. When performing experimental irradiations, determining the particle-energy fluence creating the observed damage effects is of paramount importance. This work details the use of bipolar junction transistors (BJTs) as sensors for determining the particle-energy fluence in proton and neutron irradiations over a wide range of fluences. The methodology for using BJTs as displacement damage sensors is documented in ASTM E1855: *Standard Test Method for Use of 2N2222A Silicon Bipolar Transistors as Neutron Spectrum Sensors and Displacement Damage Monitors* [2].

Radiation testing of electronic components, circuits, and systems utilizes laboratory-based radiation sources with characteristics that can vary significantly. Consistent and transferable measurement techniques for characterizing the particle fluence received by the device under test (DUT) are needed. A direct technique for measuring 1-MeV equivalent neutron fluence (1-MeV(Si)-Eqv.-n/cm^2) is based on measurement of current gain degradation due to displacement damage in silicon BJTs [3]. The technique offers several benefits over traditional dosimetry methods such as active detector measurements and neutron activation analysis (NAA). [2] [4]. The use of a bipolar displacement damage sensor is especially advantageous when seeking fluence and energy spectrum information, and/or when NAA is not feasible, typically due to a field-perturbing test object, availability of fission foils, low fluences, or restricted irradiation volumes [4] [5] [6].

Displacement damage occurs when lattice atoms are knocked out of crystalline lattice locations by energetic particle collisions that lead to the subsequent formation of stable lattice defect sites and clusters. Defect centers act as recombination states that lead to Shockley-Read-Hall recombination and decrease the minority carrier lifetime [7]. The Messenger-Spratt relationship (eq. 1) describes the reduction in minority carrier lifetime with particle fluence, which is measured as a decrease in current gain, or an increase in base current [8].

$$K_p \, \Phi_p = \frac{1}{h_{FE,\Phi}} - \frac{1}{h_{FE}} = \frac{\Delta I_B}{I_{C,1\ mA}} \qquad (1)$$

Here h_{FE} is the initial current gain (I_C/ I_B), $h_{FE,\Phi}$ is the current gain after irradiation (*FE* refers to the current gain being measured in a common, or fixed, emitter configuration with a constant voltage from emitter to collector), ΔI_B is the excess base current, $I_{C,1\ mA}$ is the collector current (current gain is

Manuscript submitted July 14, 2017.

This work was supported by Sandia National Laboratories. Sandia National Laboratories is a multimission laboratory managed and operated by National Technology and Engineering Solutions of Sandia, LLC, a wholly owned subsidiary of Honeywell International, Inc., for the U.S. Department of Energy's National Nuclear Security Administration under contract DE-NA0003525.

A. M. Tonigan, E. J. Parma, and P. J. Griffin are with Sandia National Laboratories, Albuquerque, NM 87123 USA.

A. M. Tonigan, C. N. Arutt, D. M. Fleetwood, and R. D. Schrimpf are with the Department of Electrical Engineering and Computer Science, Vanderbilt University, Nashville, TN 37212 USA (e-mail: andrew.m.tonigan@vanderbilt.edu; amtonig@sandia.gov).

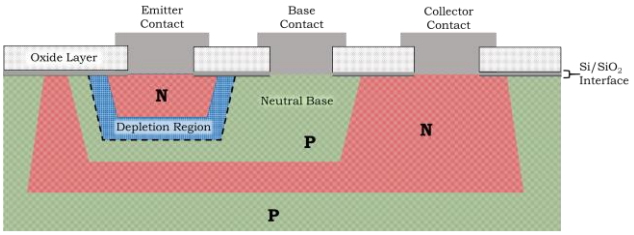

(a).

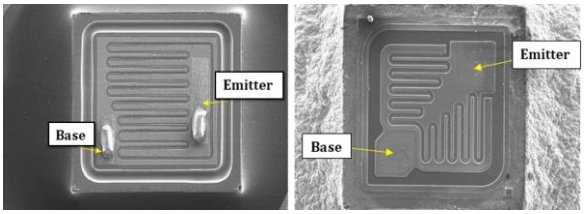

(b).

Fig. 1: (a) Bipolar *npn* device illustrative cross-section. Displacement damage effects are most significant in the neutral base and emitter-base depletion regions; total ionizing dose effects appear in the oxide layer over the base and at the silicon/silicon dioxide interface. (b) Scanning electron microscope images of the 2N1486 (left) and 2N2222 transistors (right). The feature sizes of each look similar above; however, the 2N1486 transistor is magnified ~3 times.

taken at 1 mA for each device), K_p is the particle-energy specific displacement damage factor, and Φ_p is the particle fluence received by the DUT. The current gain measurement at a collector current of 1 mA is in the linear region for forward-active biasing of each device, and no current injection annealing has observed with the devices operating up to 10 mA, making 1 mA a reliable and convenient reference point for each (vertical line in Fig. 2). The Messenger-Spratt relationship is used in the bipolar displacement damage sensor methodology by calibrating the damage factor of a particular type of device with a known, well-characterized, particle-fluence irradiation, and then using the determined damage factor to predict, or measure, the fluence received in a separate test irradiation [2]. The transistors in this work exhibit a sensitive range over many orders of magnitude of particle fluence from as low as 1 x 10^{10} 1-MeV(Si) eqv. n/cm^2 to as high as 1 x 10^{15} 1-MeV(Si) eqv. n/cm^2.

In addition to displacement damage, bipolar devices can experience current gain degradation due to ionizing radiation dose, i.e., with exposure to gamma rays and charged particles (i.e., protons, heavy ions) [9] [10] [11] [12]. A screening technique presented by Arutt et al., provides a path to take advantage of the benefits of proton irradiations to create displacement damage and compensate for the effects of ionizing radiation [13]. The technique uses the concept of non-ionizing energy loss to correlate the results to what one would obtain in neutron irradiations. Methods are presented for this process that involve quantifying the device response to ionizing dose from an x-ray or gamma irradiation and then removing its equivalent contribution to degradation from the response in a proton irradiation. Fig. 1a shows a cross-section of a simplified *npn* bipolar transistor with the primary regions of interest for total ionizing dose and displacement damage effects, and Fig. 1b shows die photos of the low and high fluence-sensitivity devices, the 2N1486 and 2N2222 transistors, respectively. A third transistor, the 2N2484, has a cut-off frequency of 60 MHz that lies between the 2N1486 and 2N2222 transistor cut-off frequencies, which are 1.2 and 300 MHz, respectively. The transistor cut-off frequencies correlate with base-width and fluence sensitivity.

II. Experimental Methods

Experimental irradiations were performed at the Sandia National Laboratories (SNL) Annular Core Research Reactor (ACRR) and Gamma Irradiation Facility (GIF) as well as the Vanderbilt University (VU) low-energy Pelletron particle accelerator and ARACOR model 4100 x-ray irradiator. 2N2222, 2N1486, and 2N2484 commercial-off-the-shelf (COTS) discrete *npn* bipolar transistors were purchased from Microsemi with no special instructions (e.g., not single die/single batch). Construction analysis was performed on the 2N2222 and 2N1486 transistors, showing a significant difference in base-width (Fig. 1b). The larger base-width device is two orders of magnitude more sensitive in neutron irradiations [5].

To observe current gain degradation ($\Delta {I_C}/{I_B}$), Gummel plots are obtained with devices connected in a common-emitter circuit before and after irradiation (log I_c, I_b vs. V_{BE}). To prevent ongoing annealing of displacement damage at room temperature from introducing a time-dependence of current gain measurements, a stabilization anneal of 80 °C for 2 hours is performed prior to post irradiation measurements (the recommended conditions suggested in ASTM E1855-15) or, if necessary, a fixed readout time. Gummel plots were obtained at SNL on a HP 4156 parameter analyzer with a fixed-temperature anodized-aluminum mounting block. At VU, a HP 4142 parameter analyzer was used in a climate controlled basement laboratory (± 2 °C). The dependence of current gain measurements on temperature has been previously established to be less than 0.5% per degree Celsius [5]. The Gummel plots are taken with the collector biased to 10 V and the emitter-base swept with rapid pulse times (~3 ms) through the forward active region up to 1 V, with maximum compliance current set at 10 mA. An example Gummel plot for each device before and after radiation-induced degradation is shown in Figs. 2a-c.

The ACRR at SNL is a pool-type nuclear fission reactor with an un-modified epithermal neutron energy spectrum. A spectrum-modifying bucket made of lead and boron (LB44) is used to shield the parts during irradiation from thermal neutrons and reduce gamma radiation exposure. The large central cavity of the ACRR allows a large volume at core centerline to be irradiated with a uniform neutron flux. The neutron energy spectrum of the ACRR is well-characterized [14]. Monitor dosimetry is calibrated with National Institute of Standards and Technology (NIST) traceable neutron sources periodically with measurement uncertainty between 4%-12% depending on activation fluence and the time delay until measurement. Traditional fluence measurement is performed with NAA of sulfur tablets and nickel foils [15] [16]. Thermoluminescent

dosimeters (TLDs) are also incorporated near DUTs to monitor gamma radiation dose [17].

The VU Pelletron accelerator [18] can be operated at proton energies up to 4 MeV, and has a uniform beam diameter of approximately one inch, allowing for only a limited number of parts to be irradiated at one time. At the radiation effects beam port end station, a custom vacuum chamber with various cable feedthroughs (e.g., BNC, SMA, fiber) houses an adjustable stage for electronic part irradiations. Traditional fluence measurements are performed with surface barrier detectors that measure Rutherford backscattering (RBS) from gold foils with ~10% measurement uncertainty. The BJTs irradiated at VU were delidded to prevent attenuation of the proton beam.

The irradiation procedure at ACRR closely follows the standard test method, with large batches of BJT sensors being irradiated in a calibration environment and subsets used in test irradiations. The restricted test volume of the Pelletron did not allow for large batch calibration irradiations. Instead of observing the response of a large group of transistors to a single irradiation, at the Pelletron a small set of device responses were recorded at many fluences. For this reason, a fixed readout time is used for the Pelletron irradiation data presented below. For a limited number of devices, the ASTM stabilization anneal was performed after 4-MeV proton irradiations that yielded comparable fluence sensor measurements but decreased the damage factor (the stabilization anneal recovers a portion of the degraded gain, decreasing the excess base current).

The ACRR and VU Pelletron deliver both ionizing and non-ionizing radiation dose to the DUTs. The ACRR LB44 environment contributes approximately 1.35 x 10^{-13} krad(SiO_2) ionizing dose per 1-MeV(Si) eqv. n/cm^2 (15% of the ionization is due to direct neutron ionization, 60% prompt gamma, and 25% delayed fission product gamma) [14]. The 4-MeV protons produced by the Pelletron contribute 1.16 x 10^{-9} krad(SiO_2) ionizing dose per 4-MeV proton/cm^2 [13].

To compensate for ionizing dose contributions to current gain degradation, each part was irradiated with cobalt-60 high energy gamma rays and 10-keV x-rays. Cobalt-60 gamma rays (1.17 MeV and 1.33 MeV) closely resemble the ionizing dose environment of a nuclear reactor (ACRR LB44's average prompt gamma energy is 1.62 MeV); whereas, the secondary electrons from 10-keV x-rays approximate the stopping power of low energy protons [13] [19] [20]. The ARACOR x-ray irradiator at VU is used to produce 10-keV x-rays on a uniform target area only slightly larger than the Pelletron uniform beam size (~two-inch diameter) while the GIF cobalt-60 source has multiple large uniform irradiation locations.

To remove the contribution to current gain degradation by ionizing dose effects and isolate displacement damage effects eq. 2 is used (following [13]). The charge yield ratio (CYR) is used to adjust the excess base current from the ionizing dose created by 20-MeV protons to that of 4-MeV protons. 20-MeV protons are considered to have equivalent total ionizing dose (TID) to 10-keV x-rays. The value used in this work for CYR is 0.54 from [13] following data from [20] [21].

$$\Delta I_{B(DD,protons)} = \Delta I_{B(total,protons)} - \left(\Delta I_{B(TID,X-rays)} \times CYR\right) \quad (2)$$

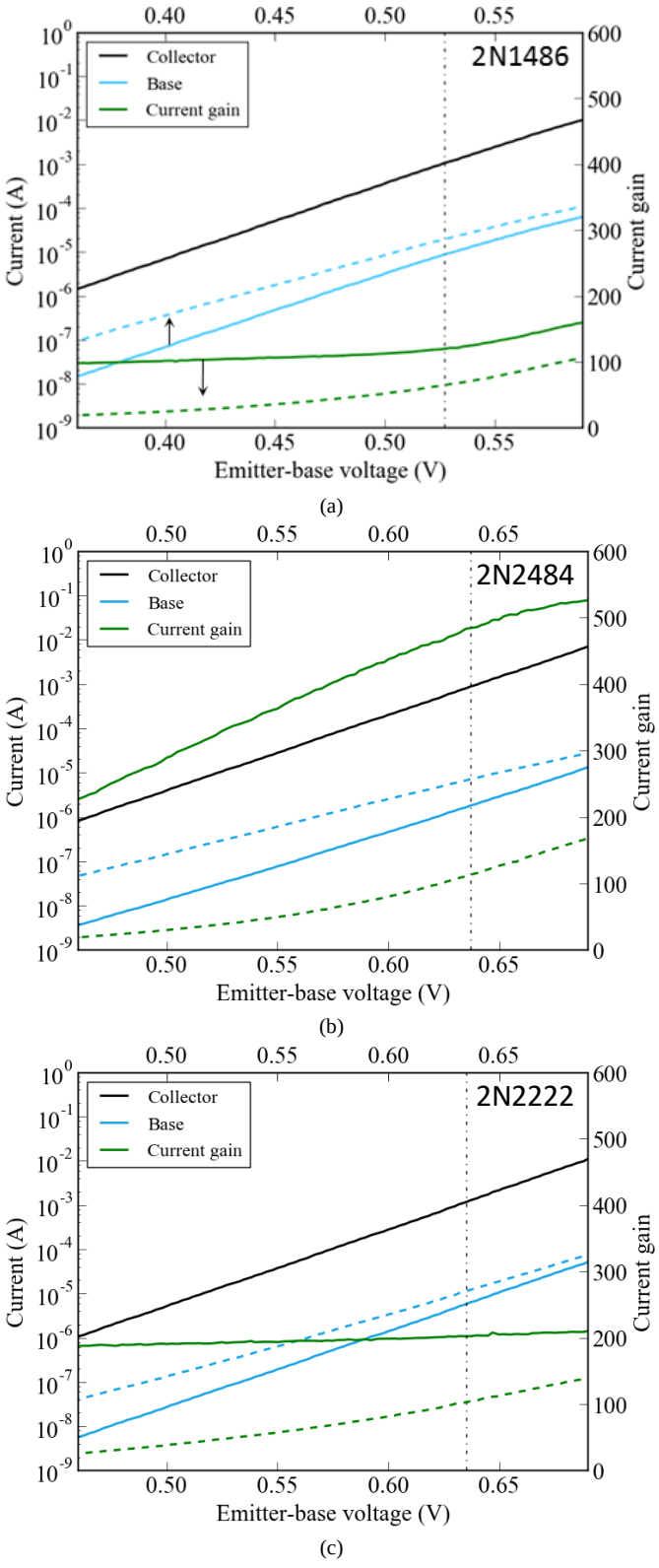

Fig. 2. Gummel and current gain plots for the three *npn* bipolar device types used in this work. The 2N2222 (a), 2N2484 (b), and 2N1486 (c) transistors are shown before (solid line) and after (dashed line) current gain degradation from particle irradiation. The 2N2484 is a higher current gain device than the other two. The dashed vertical line is placed at the reference collector current value of 1 mA.

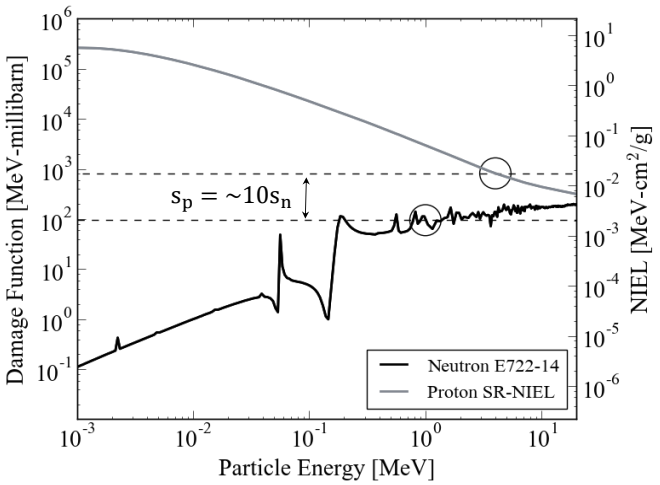

Fig. 3. Damage function versus particle energy for proton and neutron impingent on silicon. Corresponding NIEL (s_p or s_n) is plotted on the right axis. 1-MeV(Si) eqv. neutron damage is circled at a value of 95 MeV-mb and 4-MeV(Si) protons at a value of 818 MeV-mb. These values correspond to NIEL values of 2.04 x 10^{-3} MeV cm^2/g and 1.75 x 10^{-2} MeV cm^2/g and a 4-MeV proton to 1-MeV(Si) neutron NIEL ratio of 8.6. The neutron damage function is from ASTM E722-14 [3] and proton damage function from SRIM [22]. A NIEL value is obtained with MRED of 1.42 x 10^{-2} MeV cm^2/g, producing a NIEL ratio of 6.96 [13].

Non-ionizing energy loss (NIEL) calculations are proposed to screen 1-MeV(Si) eqv. neutron sensitivity with 4-MeV proton irradiations in [13]. The merits of using NIEL are addressed in the discussion section. NIEL for 4-MeV protons is 1.42 x 10^{-2} MeV-cm^2/g and 2.04 x 10^{-3} MeV-cm^2/g for 1-MeV(Si) eqv. neutrons [13]. This results in a NIEL ratio between the two particles of approximately 7. Fig. 3 shows the energy dependence of NIEL for proton and neutrons as well as the corresponding damage function. The neutron(Si) curve is taken from the dataset in E722: *Characterizing Neutron Fluence Spectra in Terms of an Equivalent Monoenergetic Neutron Fluence for Radiation-Hardness Testing of Electronics.* The proton(Si) curve in Fig. 3 is derived from screened-relativistic nuclear stopping power calculations for pure Si [22]. The Monte Carlo Radiative Energy Deposition (MRED) tool is used in [13] to provide a more accurate NIEL calculation for a silicon bipolar device.

III. Experimental Results

In Figs. 4a-c the linear change in reciprocal current gain, or increase in base current at a constant collector current, is shown for all three device types. Each figure contains corrections for the ionizing dose received during the proton irradiations (accounting for 10% - 20% of current gain degradation). The 2N2222 and 2N2484 transistors have damage factor ratios close to the calculated NIEL ratios for 4-MeV protons to 1-MeV(Si) eqv. neutrons. The 2N2222 and 2N2486 damage factor ratios are 7.8 and 6.1 (Figs. 4b-c), respectively, and the calculated NIEL ratio values are 6.96 (MRED) and 8.6 (SRIM). Ionizing dose corrections for the neutron irradiations in LB44 were negligible. The 2N1486 shows enhanced sensitivity to 4-MeV proton irradiations with a damage factor ratio of 15.3 after

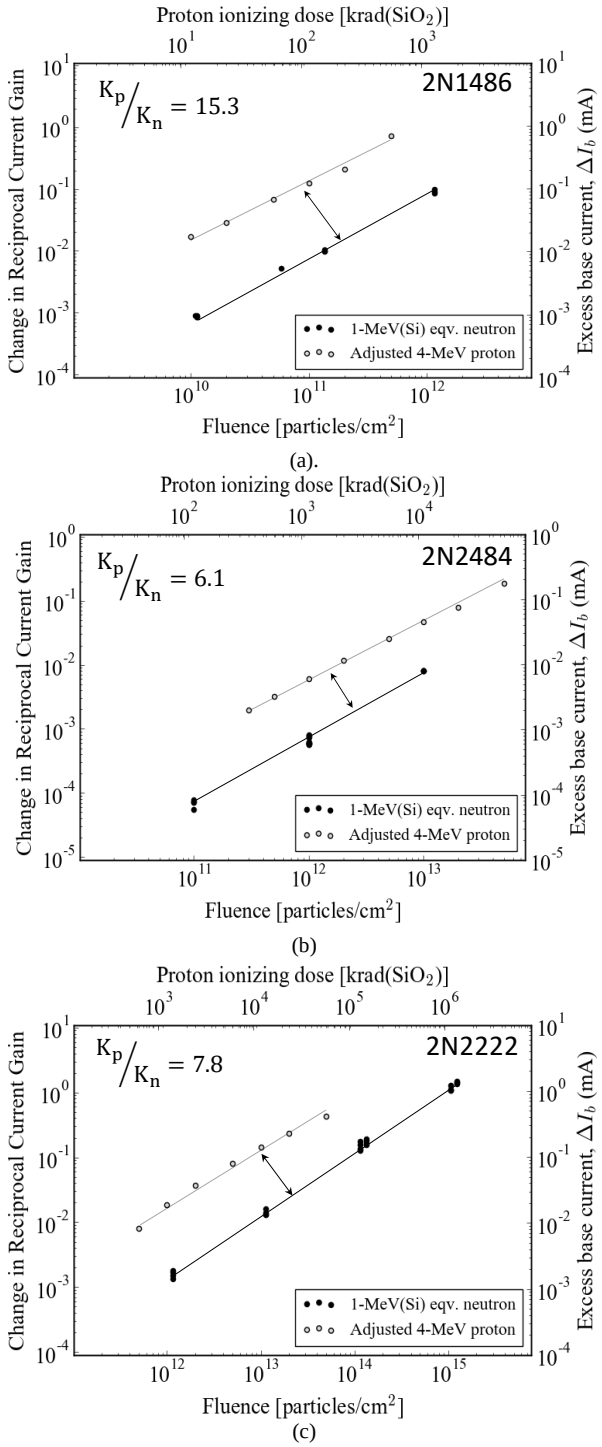

Fig. 4. The change in reciprocal current (or increase in excess base current) with particle fluence for (a). 2N1486, (b). 2N2484, and (c). 2N2222 transistors irradiated with to 4-MeV protons and 1-MeV(Si) eqv. neutrons. Each data set exhibits linear response with fluence. A linear relationship plotted on a log-log plot will always have a slope of 1 (i.e. $\ln(y) = B\ln(x)$ with $B = 1$). The ionizing dose equivalence of 4-MeV protons is plotted along the top x-axis. The damage factor ratio for each device type is displayed on the figure. The largest base-width device (the 2N1486 transistor) experiences the greatest enhanced degradation with 4-MeV proton bombardment compared to 1-MeV(Si) eqv. neutrons.

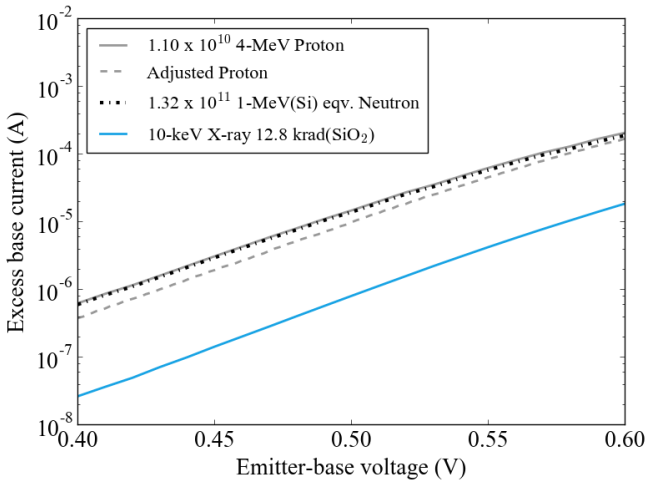

Fig. 5. Excess base current vs. base-emitter applied voltage for two representative 2N1486 transistors irradiated by an order-of-magnitude greater fluence of neutrons in ACRR (LB44) than 4-MeV protons. The excess base current from a 10-keV x-ray irradiation is displayed at an equivalent dose that corresponds to that of the 4-MeV protons. The ideality factor of the proton-irradiated device is greater than that of the neutron-irradiated device (reduced slope). This effect is most likely due to an increased contribution of recombination in the emitter-base depletion region (n = 2), an area that spreads with increased oxide trapped charge associated with TID.

ionizing dose correction. This likely indicates an increased sensitivity to combined displacement damage and ionizing dose effects along its significantly longer Si/SiO_2 interface above the base and emitter-base depletion region [23]. Ionizing dose correction improved the agreement with NIEL for the 2N1486. Before ionizing dose correction, the 2N1486 damage factor ratio would be 17.6.

Proton displacement damage sensor results for each device type are compared to the RBS traditional measurement in Table I. The results obtained provide evidence for the use of displacement damage sensors for proton irradiations, but the limited sample size (n = 9) motivates further investigation of results with a larger sample size. A high level of damage sensitivity is observed for 4-MeV protons with the 2N1486 transistor, similar to what was previously reported [5]. The uncertainties in Table I are based on uncorrelated contributions from the uncertainty in the current gain measurement and the calibrated reference fluence uncertainty (the single particle energy of 4-MeV removes the need to include spectral conversion uncertainty that is needed in a 1-MeV(Si) eqv. measurement).

Fig. 5 shows the excess base current introduced by particle and ionizing dose irradiations in the 2N1486. A fluence ratio between proton and neutron irradiations of approximately an order-of-magnitude results in overlapping excess base current measurements. The increased current ideality factor associated with the proton and ionizing dose irradiations indicates increased recombination in the emitter-base depletion region bulk and/or at the interface [24]. The ionizing dose response can vary significantly between individual devices, likely due to differences in oxide thickness and interface quality.

The efficacy of screening displacement damage sensitivity can be examined with the following prediction for the 2N1486: If the 2N1486 experiences substantial current gain degradation

TABLE I
TID COMPENSATED PROTON DISPLACEMENT DAMAGE SENSOR MEASUREMENTS COMPARED WITH RBS MEASUREMENT

RBS	2N1486
2.47×10^{10} ± 10%	2.56×10^{10} ± 10.5%
5.54×10^{10} ± 10%	5.38×10^{10} ± 10.5%
1.06×10^{11} ± 10%	8.04×10^{10} ± 10.5%
2.07×10^{11} ± 10%	1.33×10^{11} ± 10.5%
5.09×10^{11} ± 10%	6.05×10^{11} ± 10.5%
Adj. Device Damage Factor: 1.22×10^{-12}	

RBS	2N2222
2.91×10^{11} ± 10%	2.45×10^{11} ± 10.5%
5.06×10^{11} ± 10%	4.55×10^{11} ± 10.5%
1.02×10^{12} ± 10%	8.44×10^{11} ± 10.5%
2.07×10^{12} ± 10%	2.07×10^{12} ± 10.5%
5.05×10^{12} ± 10%	4.93×10^{12} ± 10.5%
1.01×10^{13} ± 10%	1.18×10^{13} ± 10.5%
Adj. Device Damage Factor: 2.73×10^{-14}	

RBS	2N2484
1.02×10^{12} ± 10%	1.20×10^{12} ± 10.5%
2.02×10^{12} ± 10%	2.59×10^{12} ± 10.5%
5.05×10^{12} ± 10%	5.91×10^{12} ± 10.5%
1.01×10^{13} ± 10%	1.12×10^{13} ± 10.5%
2.01×10^{13} ± 10%	1.90×10^{13} ± 10.5%
5.01×10^{13} ± 10%	5.17×10^{13} ± 10.5%
Adj. Device Damage Factor: 1.36×10^{-15}	

(~50%) with 4-MeV proton irradiation at a fluence of approximately 1×10^{10}, a NIEL ratio of approximately 10 would predict that a similar level of current gain degradation would occur from 1-MeV(Si) eqv. neutrons at a fluence of 1×10^{11}. Fig. 5 contains data supporting this prediction, with both devices having experienced ~50% current gain degradation.

IV. DISCUSSION

The use of BJTs as displacement damage sensors in neutron radiation effects testing is preferable over traditional NAA monitor foil dosimetry when a high fidelity spectral determination does not exist due to difficulty of incorporating the variety of sensors needed to make an adequate spectral determination into an experiment. Although this issue is not significant for modern day proton irradiation facilities (Pelletrons, cyclotrons, etc.), there is interest in correlating results between different displacement damage irradiation sources [25], and the displacement damage sensor methodology enables a fluence measurement to be taken in multiple environments with the same technique.

Proton irradiation facilities offer several benefits over neutron facilities. This is primarily because proton irradiations do not lead to neutron activation reactions that can become an issue when parts become radioactive and radiation protection concerns prevent access for variable durations. The precise

control of irradiation conditions (particle, energy, duration, etc.) is also improved upon that which is available from a nuclear reactor based irradiation source. The ability to completely "turn off" the radiation environment after an irradiation enables measurements to be performed immediately after irradiation without the background noise introduced by radioactive decay in a nuclear reactor environment. The primary drawbacks of proton irradiation facilities are the need to compensate for TID effects and the relatively limited vacuum test volume. The limited test volume restricts the possibility for full system irradiations and obtaining the statistics of a large set of device responses in a single irradiation. Also, if the neutron radiation response is desired, potential secondary reactions cannot be produced with proton irradiation and may be overlooked.

The Messenger-Spratt equation and NIEL correlation also have some limitations. Current gain degradation may not follow the Messenger-Spratt equation if there are substantial combined effects of displacement damage and ionizing dose [23]. The original Messenger-Spratt equation also does not properly treat recombination occurring in the emitter-base depletion region, leading Barnaby et al. to develop a more complete formalism in 2016 [26]. The inclusion of the modifications to the Messenger-Spratt equation is particularly important at low bias, but is not a significant factor at the reference point used in this work at medium/high biases.

Damage factors typically scale from one particle-energy to another based on the calculated NIEL for the particle-energy species [7] [27]. It is a straightforward approach to a complex phenomenon. Messenger et al. provide guidance about its limitations [28]. One complication arises due to differences in the energy deposition of protons and heavy ions. Protons and heavy ions tend to deposit most of their energy near end of range (i.e., Bragg peak). If the target region thickness is large compared to the incident particle range, non-uniform damage can occur and deviation from NIEL predictions is expected. The device dimensions of the 2N1486 transistor are approaching the region where range can become an issue and non-uniform damage can occur. The 2N2222 and 2N2484 transistors should not experience significant issues related to non-uniformity.

V. Conclusions

The use of BJTs as displacement damage sensors in a nuclear reactor and proton environment is effectively demonstrated and confirms that 4-MeV proton irradiations can be used to estimate the effects of 1-MeV(Si) eqv. neutron-induced displacement damage. Using calculated NIEL provides a good order-of-magnitude correlation between the displacement damage created by protons and neutrons. Ionizing dose correction improves the agreement with NIEL. The high level of damage sensitivity of the large base-width device, the 2N1486, is observed with 4-MeV protons irradiation.

VI. Acknowledgements

The authors would like to thank the support staff at SNL and VU for their assistance with this work.

VII. References

[1] E. P. Wigner, "Theoretical physics in the metallurgical laboratory of chicago," *J. Appl. Phys.*, vol. 17, no. 11, pp. 857-863, Nov. 1946.

[2] "E1855-15: Standard test method for use of 2N2222A silicon bipolar transistors as neutron spectrum sensors and displacement damage monitors," *ASTM International*, 2015.

[3] "E722-14: Standard practice for characterizing neutron fluence spectra in terms of an equivalent monoenergetic neutron fluence for radiation-hardness testing of electronics," *ASTM Interational*, 2014.

[4] J. G. Kelly, P. J. Griffin, and T. F. Luera, "Use of silicon bipolar transistors as sensors for neutron energy spectra determinations," *IEEE Trans. Nucl. Sci.*, vol. 38, no. 6, pp. 1180-1186, Dec. 1991.

[5] A. M. Tonigan, E. J. Parma, and W. J. Martin, "The development of high sensitivity neutron displacement damage sensor," *IEEE Trans. Nucl. Sci.*,vol. 64, no. 1, p. 346-352, Jan. 2017.

[6] M. H. Sparks, T. M. Flanders, J. G. Williams, J. G. Kelly, W. W. Sallee, M. Roknizadeh, and J. L. Meason, "Energy dependence of neutron damage in silicon bipolar transistors," *IEEE Trans. Nucl. Sci.*, vol. 36, no. 6, pp. 1904-1911, Dec. 1989.

[7] J. R. Srour, "Review of displacement damage effects in silicon devices," *IEEE Trans. Nucl. Sci.*, vol. 50, no. 3, pp. 653-670, Jun. 2003.

[8] G. L. Messenger and J. P. Spratt, "The effects of neutron irradiation on germanium and silicon," *Proceedings of the IRE*, vol. 46, pp. 1038-1044, Jun. 1958.

[9] H. J. Barnaby, R. D. Schrimpf, A. L. Sternberg, V. Berthe, C. R. Cirba, and R. L. Pease, "Proton radiation response mechanisms in bipolar analog circuits," *IEEE Trans. Nucl. Sci.*, vol. 48, no. 6, pp. 2074-2080, Dec. 2001.

[10] R. L. Pease, "Total ionizing dose effects in bipolar devices and circuits," *IEEE Trans. Nucl. Sci.*, vol. 50, no. 3, pp. 539-551, Jun. 2003.

[11] D. M. Fleetwood, "Total ionizing dose effects in MOS and low-dose-rate-sensitive linear-bipolar devices," *IEEE Trans. Nucl. Sci.*, vol. 60, no. 3, pp. 1706-1730, Jun. 2013.

[12] E. W. Enlow, R. L. Pease, W. E. Combs, R. D. Schrimpf, and R. N. Nowlin, "Response of advanced bipolar processes to ionizing radiation," *IEEE Trans. Nucl. Sci.*, vol. 38, no. 6, pp. 1342-1351, Dec. 1991.

[13] C. N. Arutt, K. M. Warren, R. D. Schrimpf, R. A. Weller, J. S. Kaupplila, J. D. Rowe, A. L. Sternberg, R. A. Reed, D. R. Ball, and D. M. Fleetwood, "Proton irradiation as a screen for displacement damage sensitivity in bipolar junction transistors," *IEEE Trans. Nucl. Sci.*, vol. 62, no. 6, pp. 2498-2504, December 2015.

[14] E. J. Parma, T. J. Quirk, L. L. Lippert, P. J. Griffin, G. E. Naranjo, and S. M. Luker, "Radiation characterization summary: ACRR 44-inch lead-boron bucket located in the central cavity on the 32-inch pedestal at the core centerline," SAND 2013-3406, Albuquerque, NM, Apr. 2013.

[15] "E264-13: Standard test method for measuring fast-neutron reaction rates by radioactivation of nickel," *ASTM International*, 2013.

[16] "E265-15: Standard test method for measuring reaction rates and fast-neutron fluences by radioactivation of sulfur-32," *ASTM International*, 2015.

[17] "E2450-16: Standard practice for application of thermoluminescence-dosimetry (TLD) systems for determining absorbed dose in radiation-hardness testing of electronic devices," *ASTM International*, 2016

[18] M. W. McCurdy, M. H. Mendenhall, R. A. Reed, B. R. Rogers, R. A. Weller, and R. D. Schrimpf, "Vanderbilt Pelletron - Low energy protons and other ions for radiation effects on electronics," *IEEE REDW*, pp. 146-151, Jul. 2015.

[19] P. Paillet, J. R. Schwank, M. R. Shaneyfelt, V. Ferlet-Cavrois, R. L. Jones, O. Flament, and E. W. Blackmore, "Comparison of charge yield in MOS devices for different radiation sources," *IEEE Trans. Nucl. Sci.*, vol. 49, no. 6, pp. 2656-2661, Dec. 2002.

[20] J. R. Schwank, M. R. Shaneyfelt, P. Paillet, D. E. Beutler, V. Ferlet-Cavrois, B. L. Draper, R. A. Loemker, P. E. Dodd, and F. W. Sexton, "Optimum laboratory radiation source for hardness assurance testing," *IEEE Trans. Nucl. Sci.*, vol. 48, no. 6, pp. 2152-2157, Dec. 2001.

[21] T. R. Oldham, "Analysis of damage in MOS devices for several radiation environments," *IEEE Trans. Nucl. Sci.*, vol. 31, no. 6, pp. 1236-1241, Dec. 1984.

[22] J. F. Ziegler, "SRIM-2013 [Online]," Available: www.srim.org.

[23] H. J. Barnaby, S. K. Smith, R. D. Schrimpf, D. M. Fleetwood, and R. L. Pease, "Analytical model for proton radiation effects in bipolar devices," *IEEE Trans. Nucl. Sci.*, vol. 49, no. 6, pp. 2643-2649, Dec. 2002.

[24] S. L. Kosier, R. D. Schrimpf, R. N. Nowlin, D. M. Fleetwood, R. L. Pease, M. DeLaus, W. E. Combs, A. Wei, and F. Chai, "Charge separation for bipolar transistors," *IEEE Trans. Nucl. Sci*., vol. 40, no. 6, pp. 1276-1285, Dec. 1993.

[25] E. Bielejec, G. Vizkelethy, N. R. Kolb, D. B. King, and B. L. Doyle, "Damage equivalence of heavy ions in silicon bipolar junction transistors," *IEEE Trans. Nucl. Sci.*, vol. 53, no. 6, pp. 3681-3686, Dec. 2006.

[26] H. J. Barnaby, R. D. Schrimpf, K. F. Galloway, X. Li, J. Yang, and C. Liu, "Displacement damage in bipolar junction transistors: Beyond Messenger-Spratt," *IEEE Trans. Nucl. Sci.*, vol. 64, no. 1, pp. 149-155, Jan. 2017.

[27] G. P. Summers, E. A. Burke, C. J. Dale, E. A. Wolicki, P. W. Marshall, and M. A. Gehlhausen, "Correlation of particle-induced displacement damage in silicon," *IEEE Trans. Nucl. Sci.*, vol. 34, no. 6, pp. 1134-1139, Dec. 1987.

[28] S. R. Messenger, E. A. Burke, G. P. Summers, and R. J. Walters, "Limits to the application of NIEL for damage correlation," *IEEE Trans. Nucl. Sci.*, vol. 51, no. 6, pp. 3201-3206, Dec. 2004.